JOURNAL OF MATERIALS SCIENCE 11 (1976) 89–96

Electron spin resonance linewidths of Fe^{3+} in magnesium oxide

J. S. THORP, R. A. VASQUEZ, C. ADCOCK, W. HUTTON
Department of Applied Physics and Electronics, University of Durham, UK

Electron spin resonance linewidths of Fe^{3+} in single crystal MgO at 9 GHz were examined experimentally and theoretically for a range of Fe^{3+} concentration. In contrast to the behaviour expected from dipolar broadening the experimental derivative peak-to-peak linewidth for the $\frac{1}{2} \leftrightarrow -\frac{1}{2}$ transition, about 0.6 mT at 77 K and a polar angle of 0°, was independent of concentration from 140 to 8500 ppm. The calculated dipolar linewidths greatly exceeded those observed and values of the ratio of moments $M_4^{1/4}/M_2^{1/2}$ derived from the experimental data lay between 1.33 and 1.48. Optical examination, coupled with heat-treatment experiments, confirmed that the predominant valency state present was Fe^{3+}. The data suggested that Fe^{3+} entered the lattice substitutionally, occupying magnesium sites, and that the linewidths were determined by exchange narrowing over the whole concentration range examined.

1. Introduction

Magnesium oxide is widely used commercially, often in its fused or powdered forms, either purely for its refractory properties or, more specifically, as an electrically insulating refractory material. In the latter context, which has been the subject of much work over the past two decades [1, 2], questions still remain as to the possible role of impurities in influencing the electrical properties and breakdown at high temperatures. As part of a further study of some of these effects an investigation has been made of the electron spin resonance behaviour of a number of doped magnesias in an attempt to establish the location of the dopant atoms and so provide specimens of known structural characteristics on which electrical conductivity and dielectric loss measurements might subsequently be made. Some electron spin resonance data on magnesium oxide doped with transition element ions, for example Fe, Co, Cr and Ni has previously been reported in the literature [3] and the characteristic parameters of the spin-Hamiltonian calculated for crystalline fields having cubic symmetry. There is, however, little detailed information available either on the question of the sites actually occupied by the dopant atoms or on the nature of the interactions between the latter. Information of this nature has recently been obtained in several materials, including doped calcium tungstate [4, 5] and alumina [6, 7], by making a comparison between the observed esr linewidths and those predicted from dipolar broadening. It was decided to adopt a similar approach with iron-doped magnesia. This paper presents the results of the linewidth comparison made for the $\frac{1}{2} \leftrightarrow -\frac{1}{2}$ transition of Fe^{3+}.

2. Experimental techniques

The doped single crystals on which measurements were made were obtained from W. & C. Spicer Ltd (Cheltenham), having been grown by electrofusion using pure powdered ferric oxide and pure powdered magnesia as the starting materials.

The iron concentrations in the specimens examined ranged from 140 to 11 900 ppm; these had been determined by optical spectrographic analysis (Johnson–Matthey Ltd) to an accuracy of about 2%. The crystalline quality was good and neither optical examination nor X-ray back-reflection photographs, used to orient the specimens, revealed any evidence of macroscopic cracking, flaws, strain or mosaic formation. The crystals were coloured, varying from pale green at 140 ppm Fe to dark green at 11 900 ppm Fe; optical absorp-

tion spectroscopy revealed features, described in detail later, which were taken as indicative of Fe^{3+}. Visual examination showed the coloration, and hence the doping level, to be quite uniform over each of the individual specimens, which typically had dimensions of 9.8 mm x 7 mm x 2.61 mm, chosen, to suit the spectrometer cavity requirement.

The electron spin resonance measurements were made using a conventional 9 GHz spectrometer equipped with phase sensitive detection and giving output spectra in derivative form. Some difficulty was experienced in matching the spectrometer cavity. The match between the input waveguide and the cavity depended quite critically on the size of the specimen and, to a lesser extent, on the doping level and it was found necessary to incorporate a continuously variable matching unit. This consisted of a brass plunger passing through the broad face of a section of rectangular guide mounted immediately above the rectangular TE_{102} cavity, the position of the plunger could be adjusted from the cryostat head. Spectra were recorded, at both 293 and 77 K, by sweeping the magnetic field slowly through a known range. The magnetic field calibrations were obtained using a proton resonance magnetometer system in which the probe could be located exactly in the position normally occupied by the specimen.

3. Experimental results

Initial measurements were made to establish the form of the spectrum in each specimen. An example of this is shown in Fig. 1 which refers to a specimen containing 310 ppm Fe examined at 293 K. The spectrum at $\theta_H = 0°$ shows a total of five lines of which the one centred at about $g = 2$ is the most prominent. The field values at which the transitions occurred were compared with the values expected from the energy level diagram [8, 9]. There was close agreement and on this basis, and in view of the similarity between Fig. 1 and the features of the 1.15 cm region spectrum reported by Low [3], it was felt justifiable to attribute the spectrum to Fe^{3+} in octahedral sites. Some specimens showed weak additional lines which were thought to be due to impurities. Measurements of the magnetic field values at resonance for the transitions and linewidth determinations were made as functions of polar angle.

The iso-frequency plots showed that, while the $\frac{1}{2} \leftrightarrow -\frac{1}{2}$ transition was nearly isotropic, the other transitions were markedly anisotropic. The variations for the $\frac{3}{2} \leftrightarrow \frac{1}{2}$ and $-\frac{3}{2} \leftrightarrow -\frac{1}{2}$ transitions are depicted in Fig. 2. At angles near $\theta_H = 30°$ and $\theta_H = 60°$ there is overlap with the $\frac{1}{2} \leftrightarrow -\frac{1}{2}$ transition which, by contrast, was found to be much less anisotropic. Low [3] has previously reported

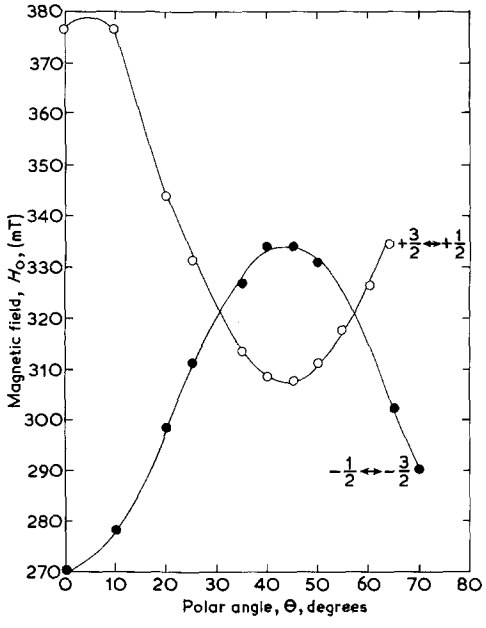

Figure 2 Isofrequency plot, $+\frac{3}{2} \leftrightarrow +\frac{1}{2}$ and $-\frac{1}{2} \leftrightarrow -\frac{3}{2}$ transitions, 9.09 GHz.

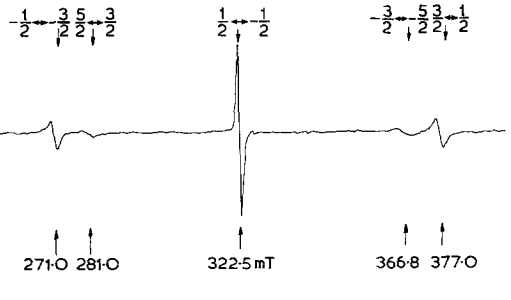

Figure 1 Esr spectrum of Fe^{3+}/MgO; room temperature, $\theta_H = 0$e, 9.10 GHz, 310 ppm Fe.

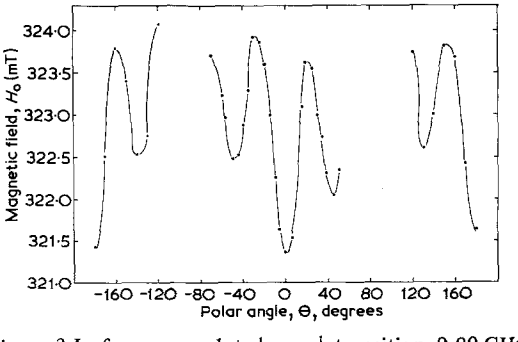

Figure 3 Isofrequency plot, $\frac{1}{2} \leftrightarrow -\frac{1}{2}$ transition, 9.09 GHz.

isotropic behaviour for the $\frac{1}{2} \leftrightarrow -\frac{1}{2}$ transition but the present measurements (Fig. 3) show that there is a small periodic variation in the resonance field which departs by up to 3 mT from its value at $\theta_H = 0°$. The pattern of variation is very similar to that reported by Toussaint and Declerck [10] who found, for the case in which the magnetic field was directed along the ⟨1 1 1⟩ axis of the crystal, changes in resonance magnetic field of up to 4 mT over a similar range of polar angle.

The $\frac{1}{2} \leftrightarrow -\frac{1}{2}$ transition was used for detailed linewidth studies, primarily because of its greater intensity. The linewidths, defined as the width between points of maximum slope, ΔH_{ms}, was obtained directly from the derivative plots. The linewidth variation with polar angle was measured. All the curves show a minimum near $\theta_H = 0°$ where the linewidth at room temperature is approximately 0.8 mT. In order to check whether there was any appreciable contribution to linewidth due to broadening caused by spin-lattice relaxation, the spectra were then recorded at 77 K. The linewidths measured were similar to those at 300 K showing that this effect was negligible. Fig. 4 illustrates the

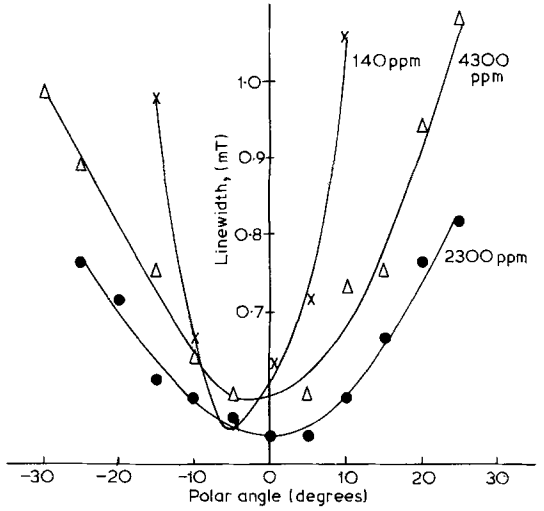

Figure 4 Linewidth variation with polar angle ($\theta_H < 30°$).

variation of linewidth with polar angle obtained at 77 K for several of the specimens; measurements at high values of θ were restricted due to the reduction in intensity of the $\frac{1}{2} \leftrightarrow -\frac{1}{2}$ transition and to difficulties with overlapping transitions but the variation appeared to be periodic.

4. Dipolar broadening

It will be assumed in this calculation that the main contribution to homogeneous line broadening is dipole–dipole interactions between Fe^{3+} ions; the magnitude of this broadening is calculated using the second moment theory of Van Vleck [11].

For like atoms the second moment, $\langle \Delta\omega^2 \rangle$, can be written

$$\langle \Delta\omega^2 \rangle = \tfrac{3}{4} S(S+1)(g^2\beta^2/\hbar)^2 \cdot n \sum_k \left[r_{jk}^{-6} (3\cos^2\theta_{jk} - 1)^2 \right] \quad (1)$$

where ω is measured in rad sec^{-1}, n is the concentration of interacting atoms, g is the Lande g-factor, β is the Bohr magneton, r_{jk} is the radius vector from the reference atom j to all the neighbouring atoms labelled over k, θ_{jk} is the angle between the radius vector and a crystallographic reference axis. The term $r_{jk}(3\cos^2\theta_{jk} - 1)^2$ can be evaluated using spherical harmonics, $Y_{l,m}$, if the form of the unit cell is known [4].

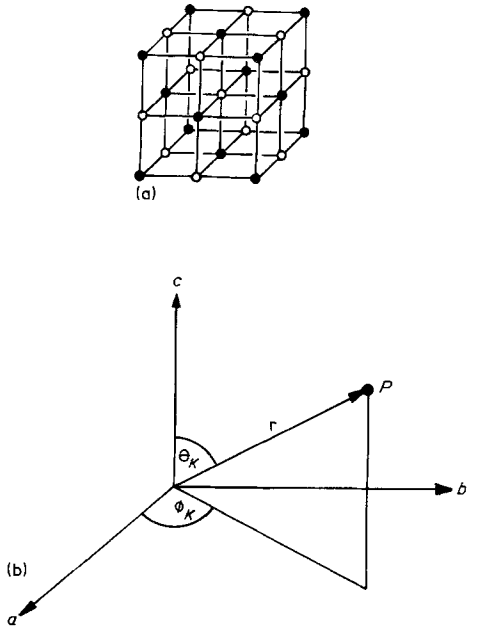

Figure 5 The magnesium oxide unit cell. (a) Atomic positions; • = magnesium, ○ = oxygen. (b) Reference axes.

The unit cell of magnesium oxide is face centred cubic having $a = 4.2112$ Å (21° C) [12] as shown in Fig. 5. The iron is expected to substitute at the magnesium sites and so a complete tabulation of these sites is needed. It is found sufficient to consider eight unit cells with the iron reference ion as a common corner because the contribution from more remote cells is negligible. The r, θ, ϕ values of all the magnesium sites are given in Table AI.

For a crystal of cubic symmetry the equation of the second moment for like atoms is:

$$\langle\Delta\omega^2\rangle = \frac{3}{4}S(S+1)(g^2\beta^2/\hbar)^2 \cdot n \left[\frac{4}{5}\sum_k (r_{jk}^{-6}) + \frac{32\pi}{35} Y^*_{4,0}(\theta_H,\phi_H)\sum_k r_{jk}^{-6} Y_{4,0}(\theta_k,\phi_k) + \frac{32\pi}{35} Y^*_{4,4}(\theta_H,\phi_H)\sum_k r_{jk}^{-6} Y_{4,4}(\theta_k,\phi_k) + \frac{32\pi}{35} Y^*_{4,-4}(\theta_H,\phi_H)\sum_k r_{jk}^{-6} Y_{4,-4}(\theta_k,\phi_k)\right] \quad (2)$$

where θ_k and ϕ_k refer the radius vector to the crystal axes while θ_H and ϕ_H refer the static magnetic field to the same axes. Because of the symmetrical properties of the crystal structure this equation reduces at $\phi_H = 0°$ (which is the case considered here) to

$$\langle\Delta\omega^2\rangle = \frac{3}{4}S(S+1)(g^2\beta^2/\hbar)^2 \cdot n \left[\frac{4}{5}\sum_k (r_{jk}^{-6}) + \frac{32\pi}{35} Y^*_{4,0}(\theta_H,\phi_H)\sum_k r_{jk}^{-6} Y_{4,0}(\theta_k,\phi_k) + \frac{64\pi}{35} Y^*_{4,4}(\theta_H,\phi_H)\sum_k r_{jk}^{-6} Y_{4,4}(\theta_k,\phi_k)\right]. \quad (3)$$

The total dipolar broadening is given by the square root of the sum of the second moments of the individual dipolar interactions. This mean square width must be converted into the peak-to-peak derivative linewidths, $\Delta H_{\rm ms}$, for comparison with experimental results. This is done using the equation

$$\Delta H_{\rm ms} = \frac{\sqrt{\langle\Delta\omega^2\rangle}}{\pi} \cdot \partial H/\partial\nu \text{ Tesla} \quad (4)$$

where the parameter $\partial H/\partial\nu$ is obtained from the experimental isofrequency plots obtained for each crystal.

For Fe^{3+}, $S = 5/2$ and $g = 2.0037$ [3] and so the atomic part of the equation can be evaluated as

$$\tfrac{3}{4}S(S+1)(g^2\beta^2/\hbar)^2 \cdot n = 7.0621 \times 10^{-25} \cdot n\,(\text{rad sec}^{-1})\,\text{cm}^6. \quad (5)$$

Using Table AII the geometrical part of the equation can be partially evaluated leading to the final equation

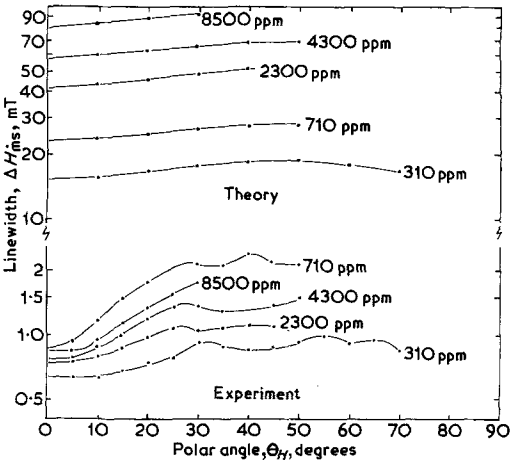

Figure 6 Linewidth versus polar angle for the $\frac{1}{2} \leftrightarrow -\frac{1}{2}$ transition.

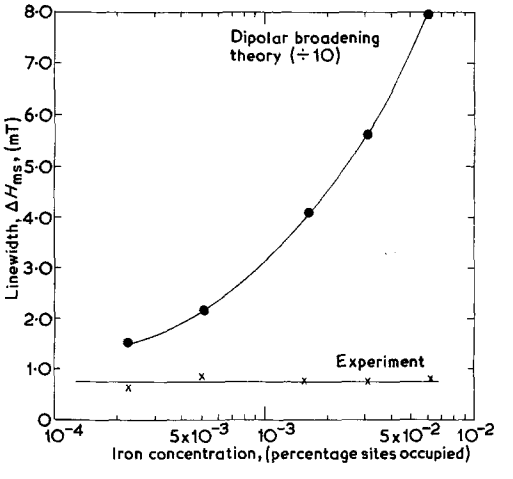

Figure 7 Variation of linewidth with concentration; $\frac{1}{2} \leftrightarrow -\frac{1}{2}$ transition, $\theta_H = 0$.

$$\langle\Delta\omega^2\rangle = 7.062 \times 10^{20} \cdot n\,[15.9184 - 5.175\,Y^*_{4,0}(\theta_H,\phi_H) - 6.218\,Y^*_{4,4}(\theta_H,\phi_H)]. \quad (6)$$

For $\phi_H = 0°$ the equation is totally real and by substituting the experimental values of n and θ_H curves of dipolar broadening as a function of polar angle can be derived. Using the transformation of Equation 4, $\Delta H_{\rm ms}$ can then be calculated and compared with experimental values. The general curves for the variation of linewidth with polar angle are given in Fig. 6. The predicted concentrated dependence of linewidth obtained on the crystals in the as grown state is shown in Fig. 7, which also gives the experimental data.

5. Discussion

Two salient features emerge from an initial comparison between the experimental results for the as grown crystals and those predicted on the basis of dipolar broadening. In the first place the predicted linewidths are about a hundred times larger than the observed linewidths; secondly, the linewidth appears to be almost concentration independent in marked contrast to the $(\text{concentration})^{1/2}$ variation expected for dipolar broadening.

The discrepancy in the magnitude of the linewidth is far greater than those encountered in other materials in which similar comparisons have been made. In ruby, for example, Grant and Strandberg [6] found that the predicted dipolar widths were some five times larger than the observed widths; in neodymium doped calcium tungstate [4] Brown *et al.* found that the predicted widths agreed closely with those observed; in double doped alumina Thorp *et al.* [7] found that the predicted widths were seven times larger than those observed and in gadolinium calcium tungstate [5] Thorp *et al.* found a similar factor. In these examples there was a reasonably good fit between the forms of the predicted and observed angular variation of the linewidth and also between the predicted and observed linewidth versus concentration variation. With the present data only the form of the angular variation of linwidth corresponds to the predictions of the dipolar model. The large numerical disparity suggested either that the values used for the Fe^{3+} concentrations were incorrect or that there was a strong narrowing mechanism such as, for example, exchange [11] or motional [13] narrowing. These possibilities, which led to some further optical and esr experiments on heat-treated specimens, are discussed below.

As regards the Fe^{3+} concentrations the figures used, obtained by spectrographic analysis, referred to the total iron content. This method of analysis did not differentiate between various valency states and consequently it was possible that although the crystals certainly contained Fe^{3+} – as shown by the esr spectra – they might also contain other states such as Fe^{2+}. There is a considerable literature on the optical absorption behaviour of Fe^{2+} and Fe^{3+} but the positive identification of species in particular lattices is not entirely straightforward. Jones [14] has reported that for Fe^{2+} in octahedral co-ordination a peak corresponding to the $T_{2g} \rightarrow E_g$ transition is observed at 970 nm, a result confirmed by Cotton and Meyers [15], and also by King *et al.* [16]. The optical behaviour of Fe^{3+} in cubic fields is well documented, e.g. Wickersheim and Lefever [17], but there is relatively little data specifically relating to MgO; Wertz *et al.* [18] however identified two peaks in iron-doped magnesia, occurring at 400 and 459 nm as due to Fe^{3+}. The optical transmission in most of the present specimens has been studied over the range 200 nm to 1000 nm using an Optica Type CF4 spectrophotometer, and over the range 600 to 1000 nm using a Grubb and Parsons Spectromaster. In the as-received state all the specimens examined showed minima at 395 nm and 462 nm (see Fig. 8), the magnitude of which increased progressively with total iron concentration. Only two specimens, those containing 2300 ppm Fe and 4300 ppm Fe respectively, gave in addition a broad minimum centred near 1000 nm (Fig. 9). We thus conclude from this optical data that while all the specimens contained Fe^{3+} only the two specimens noted above contained a detectable amount of Fe^{2+}. Further evidence was obtained from a series of heat treatment experiments. After heating in air at 1200° C for up to 30 hours the initially green

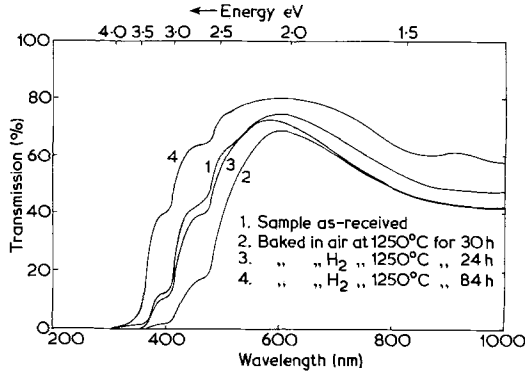

Figure 8 Optical transmission in iron-doped magnesium oxide, (2300 ppm Fe, 300 to 1000 nm).

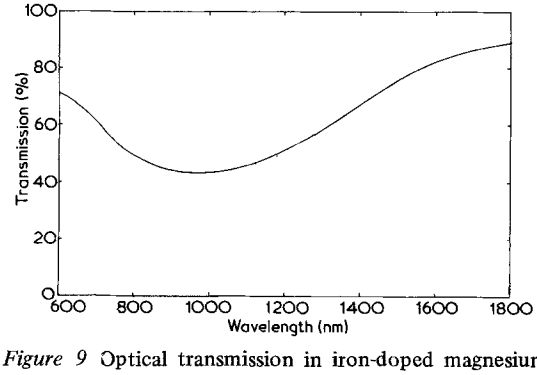

Figure 9 Optical transmission in iron-doped magnesium oxide, (2300 ppm Fe, 600 to 1800 nm).

coloured specimens turned orange; these visual changes were accompanied by changes in the optical transmission also indicated in Fig. 8. Thus it was confirmed that heating in air or oxygen increased the Fe^{3+} content, presumably at the expense of the Fe^{2+} content, and that the reverse applied after heat-treatment in hydrogen, although it was not possible to make accurate quantitative estimates of relative proportions; our optical observations fit closely with those reported previously [18].

After heat-treatment in air the intensity of the Fe^{3+} esr spectrum was, in most specimens, somewhat larger and the linewidths tended to increase but only by factors of less than two times; even in the situation where maximum conversion of Fe^{2+} into Fe^{3+} had been attempted (after prolonged heating in air) the linewidths were still very much less than the predicted values. The dipolar calculations can be used to obtain the concentration of Fe^{3+} which would have been needed to account on the dipolar model for the observed 0.8 mT linewidth. This extrapolation gives a required concentration of only about 0.5 ppm Fe^{3+}. Even allowing for a substantial percentage of the total iron content being present as species other than Fe^{3+} this extremely low value makes it very unlikely that the linewidth discrepancy could be explained purely on concentration grounds; furthermore, no explanation of the concentration independent linewidths would be afforded without an unlikely assumption that the Fe^{3+} concentration remained low and constant although the total iron content increased from 140 to 11 900 ppm.

An explanation in terms of exchange narrowing seems more likely since this would involve an interaction between ions of like species which here would be $Fe^{3+} \leftrightarrow Fe^{3+}$. Exchange line narrowing mechanisms have been examined by Van Vleck [19]. Experimental evidence for exchange narrowing is usually obtained from analysis of lineshapes and especially by comparison of moments. A review by Al'Tshuler [20] gives

$$\frac{M_4^{1/4}}{M_2^{1/2}} \gg 1$$

where M_2 and M_4 are respectively the second and fourth moments of the line as a criterion for exchange narrowing. An analysis of this type has been attempted in the following way. Each absorption lineshape was first found by numerical integration of the experimental derivative plots; these resembled that reported by Zavoisky [21] for the exchange narrowed line of $CrCl_3$ polycrystalline samples. A difficulty was encountered on the high field side of the main transition by the presence of a weak subsidiary line. This made it impossible to obtain data in the high field tail and consequently estimates of M_2 and M_4 were only made for the left-hand side of the line where the tail could be followed continuously into the background. The ratio $M_4^{1/4}/M_2^{1/2}$ was then derived and the results are summarized in Table I. The values of the ratio

TABLE I Values of the ratio $M^{1/4}/M^{1/2}$ for Fe^{3+} in single crystal MgO ($\frac{1}{2} \leftrightarrow -\frac{1}{2}$ transition, 77 K data); for comparison some of Van Vleck's data is included.

Substance	Experimental linewidth (mT)	Calculated linewidth (mT)	Ratio $M^{1/4}/M^{1/2}$
Iron-doped magnesia, Fe^{3+}/MgO			
140 ppm	0.66	10.49	1.34
310 ppm	0.63	15.56	1.36
710 ppm	0.62	23.67	1.33
2300 ppm	0.58	42.58	1.48
4300 ppm	0.63	58.44	1.42
Manganese salts, (Van Vleck's data)			
$MnCl_2$	75.0	295	1.40
$MnSO_4$	66.5	352	1.35
$MnCo_3$	46.0	446	1.43
MnF_2	47.0	702	1.39
MnS	78.0	752	1.40

are similar to the figures quoted elsewhere for other examples of exchange narrowed esr lines, e.g. in Mn^{2+} salts, Van Vleck [19]. This suggests that exchange narrowing is important, even at the lowest iron concentration (140 ppm Fe). The exchange model might also give an explanation for the concentration independent linewidths. Increasing the iron concentration will increase the number of Fe^{3+} atoms occupying sites at the minimum distance from the reference atom and so produce a stronger narrowing effect; thus the concentration independence of the linewidth is to be regarded as the maintenance of the domination of exchange narrowing over dipolar broadening at all levels of iron concentration.

On the above basis one might expect that the linewidth behaviour of the Fe^{3+} should be substantially independent of any Fe^{2+} present. The present data on heat-treated specimens supports this view; after heat-treatment in air small increases in linewidth were observed whereas after heat-treatment in hydrogen small decreases were seen. The heat-treatments were respectively such as to maximize the conversion of the iron present to

either Fe^{3+} or Fe^{2+} yet the linewidth always remained much smaller than the predicted dipolar width. We cannot rule out the possibility of some contribution to narrowing arising from motional effects, which have been invoked by Stoneham *et al.* [22] to explain the temperature dependence of the linewidth or iron group ions in MgO in the temperature range near 2 K. This mechanism, however, would involve an Fe^{3+}–Fe^{2+} interaction and, in view of the small amounts of Fe^{2+} detected in the specimens used in these experiments, seems unlikely to be a dominant factor. Thus we conclude from the linewidth experiments that the iron enters the magnesium oxide lattice substitutionally

TABLE AI Values of r, θ and ϕ for magnesium sites in eight unit cells of MgO, taking the common corner as the origin of the polar co-ordinate system (see Fig. 5).

a	b	c	r(Å)	θ°	ϕ°	a	b	c	r(Å)	θ°	ϕ°
$\frac{1}{2}$	$\frac{1}{2}$	0	2.9778	90	45	$\frac{1}{2}$	−1	$\frac{1}{2}$	5.158	65.91	296.56
$-\frac{1}{2}$	$\frac{1}{2}$	0	2.9778	90	135	$-\frac{1}{2}$	−1	$-\frac{1}{2}$	5.158	114.09	243.44
$-\frac{1}{2}$	$-\frac{1}{2}$	0	2.9778	90	225	$\frac{1}{2}$	−1	$-\frac{1}{2}$	5.158	114.09	296.56
$\frac{1}{2}$	$-\frac{1}{2}$	0	2.9778	90	315	1	$\frac{1}{2}$	$\frac{1}{2}$	5.158	65.91	26.57
0	$\frac{1}{2}$	$\frac{1}{2}$	2.9778	45	90	1	$-\frac{1}{2}$	$\frac{1}{2}$	5.158	65.91	333.43
0	$-\frac{1}{2}$	$\frac{1}{2}$	2.9778	45	270	1	$\frac{1}{2}$	$-\frac{1}{2}$	5.158	114.09	26.57
0	$\frac{1}{2}$	$-\frac{1}{2}$	2.9778	135	90	1	$-\frac{1}{2}$	$-\frac{1}{2}$	5.158	114.09	333.43
0	$-\frac{1}{2}$	$-\frac{1}{2}$	2.9778	135	270	−1	$\frac{1}{2}$	$\frac{1}{2}$	5.158	65.91	153.43
$\frac{1}{2}$	0	$\frac{1}{2}$	2.9778	45	0	−1	$-\frac{1}{2}$	$\frac{1}{2}$	5.158	65.91	206.56
$-\frac{1}{2}$	0	$\frac{1}{2}$	2.9778	45	180	−1	$\frac{1}{2}$	$-\frac{1}{2}$	5.158	114.09	153.43
$\frac{1}{2}$	0	$-\frac{1}{2}$	2.9778	135	0	−1	$-\frac{1}{2}$	$-\frac{1}{2}$	5.158	114.09	206.56
$-\frac{1}{2}$	0	$-\frac{1}{2}$	2.9778	135	180						
						1	0	1	5.956	45	0
0	0	1	4.2112	0	–	−1	0	1	5.956	45	180
0	0	−1	4.2112	180	–	1	0	−1	5.956	135	0
1	0	0	4.2112	90	0	−1	0	−1	5.956	135	180
0	1	0	4.2112	90	90	0	1	1	5.956	45	90
−1	0	0	4.2112	90	180	0	−1	1	5.956	45	270
0	−1	0	4.2112	90	270	0	1	−1	5.956	135	90
						0	−1	−1	5.956	135	270
$\frac{1}{2}$	$\frac{1}{2}$	1	5.158	35.26	45	1	1	0	5.956	90	45
$-\frac{1}{2}$	$\frac{1}{2}$	1	5.158	35.26	135	−1	1	0	5.956	90	135
$-\frac{1}{2}$	$-\frac{1}{2}$	1	5.158	35.26	225	−1	−1	0	5.956	90	225
$\frac{1}{2}$	$-\frac{1}{2}$	1	5.158	35.26	315	1	−1	0	5.956	90	315
$\frac{1}{2}$	$\frac{1}{2}$	−1	5.158	144.74	45						
$-\frac{1}{2}$	$\frac{1}{2}$	−1	5.158	144.74	135	1	1	1	7.294	54.74	45
$-\frac{1}{2}$	$-\frac{1}{2}$	−1	5.158	144.74	225	−1	1	1	7.294	54.74	135
$\frac{1}{2}$	$-\frac{1}{2}$	−1	5.158	144.74	315	−1	−1	1	7.294	54.74	225
$\frac{1}{2}$	1	$\frac{1}{2}$	5.158	65.91	63.44	1	−1	1	7.294	54.74	315
$-\frac{1}{2}$	1	$\frac{1}{2}$	5.158	65.91	116.56	1	1	−1	7.294	125.26	45
$\frac{1}{2}$	1	$-\frac{1}{2}$	5.158	114.09	63.44	−1	1	−1	7.294	125.26	135
$-\frac{1}{2}$	1	$-\frac{1}{2}$	5.158	114.09	116.56	−1	−1	−1	7.294	125.26	225
$-\frac{1}{2}$	−1	$\frac{1}{2}$	5.158	65.91	243.44	1	−1	−1	7.294	125.26	315

TABLE AII Trigonometrical parameters for the magnesium sites in eight unit cells of MgO, the origin of co-ordinates being the common corner.

r(Å)	θ_k°	ϕ_k°	N (No. of sites)	$Y_{4,0}(\theta_k, \phi_k)$	$Y_{4,4}(\theta_k, \phi_k)$	$Nr^{-6} \times 10^{45}\,cm^{-6}$	$Nr^{-6}Y_{4,0}(\theta_k, \phi_k) \times 10^{45}\,cm^{-6}$	$Nr^{-6}Y_{4,4}(\theta_k, \phi_k) \times 10^{45}\,cm^{-6}$
2.978	90	45	4	0.3174	−0.4425	5.737	1.8209	−2.5386
2.978	45	0	8	−0.3438	0.1106	11.4741	−3.9448	−1.2690
4.211	0	–	2	0.8463	0.0000	0.3586	0.3035	0.0000
4.211	90	0	4	0.3174	0.4425	0.7171	0.2276	0.3173
5.158	35.26	45	8	−0.1528	−0.04917	0.4297	−0.06494	−0.02113
5.158	65.91	26.57	16	−0.1087	−0.0861	0.8594	−0.0934	−0.0740
5.956	45	0	8	−0.3438	0.1106	0.1793	−0.0616	0.0198
5.956	90	45	4	0.3174	−0.4425	0.0897	0.0285	−0.0397
7.294	54.74	45	8	−0.3291	−0.1967	0.05313	−0.0175	−0.0105
					SUM	19.898	−1.8017	−1.0823

(occupying magnesium sites), that the predominant valency state is Fe^{3+} and that even at low concentrations there is strong exchange narrowing of the resonance lines.

Acknowledgements

R.A.V. wishes to thank the British Council and the Ford Foundation for the award of a Research Scholarship and W.H. thanks the Science Research Council for the award of a Research Studentship.

References

1. S. P. MITOFF, *J. Chem. Phys.* **31** (1959) 1261.
2. C. M. OSBURN and R. W. VEST, *J. Amer. Ceram. Soc.* **54** (1971) 428.
3. W. LOW, *Ann. N.Y. Acad. Sci.* **72** (1958) 69.
4. G. BROWN, C. J. KIRKBY and J. S. THORP, *J. Mat. Sci.* **9** (1974) 65.
5. J. S. THORP, G. BROWN and H. P. BUCKLEY, *ibid* **9** (1974) 1337.
6. W. J. C. GRANT and M. W. W. STRANDBERG, *Phys. Rev.* **135A** (1964) 727.
7. J. S. THORP and H. P. BUCKLEY, *J. Mater. Sci.* **9** (1974) 1499.
8. P. DEBYE, *Ann. Physik.* **32** (1938) 85.
9. R. DE L. KRONIG and C. J. BOUWKAMP, *Physica* **6** (1939) 290.
10. J. TOUSSAINT and C. DECLERK, *Bull. Soc. Roy. Sci. Liege* **1** (1966) 93.
11. J. H. VAN VLECK, *Phys. Rev.* **74** (1948) 1168.
12. R. W. G. WYCKOFF, "Crystal Structures", Vol. 1 (Interscience, New York, 1965).
13. P. W. ANDERSON, *Phys. Rev.* **114** (1959) 1002.
14. G. D. JONES, *ibid* **155A** (1967) 259.
15. F. A. COTTON and M. D. MEYERS, *J. Amer. Ceram. Soc.* **82** (1960) 5023.
16. R. D. KING and B. HENDERSON, *Proc. Brit. Ceram. Soc.* **9** (1967) 63.
17. K. A. WICKERSHEIM and R. A. LEFEVER, *J. Chem. Phys.* **36** (1962) 844.
18. J. E. WERTZ, G. SAVILLE, P. AUZINS and J. W. ORTON, *J. Phys. Soc. Japan* **18** Supp. II (1963) 305.
19. J. H. VAN VLECK, *Nuovo Cimento Supp.* **6** (1957) 993.
20. S. A. AL'TSHULER and B. M. KOZYREV, "Electron Paramagnetic Resonance" (Academic Press, New York, 1964).
21. Y. K. ZAVOISKY, *Sov. Fiz.* **10** (1946) 197.
22. A. M. STONEHAM, K. A. MÜLLER and W. BERLINGER, *Solid. Stat. Commun.* **10** (1972) 1005.

Received 25 April and accepted 27 May 1975.